Adsorption (2011) 17: 497–504
DOI 10.1007/s10450-010-9309-z

CO_2 adsorption on binderless activated carbon monoliths

Diana Paola Vargas · Liliana Giraldo · Joaquín Silvestre-Albero · Juan Carlos Moreno-Piraján

Received: 31 August 2010 / Accepted: 1 December 2010 / Published online: 10 December 2010

Abstract A series of activated carbon monoliths have been prepared by chemical activation of two lignocellulosic precursors, coconut shell (CACM) and African palm stones (PACM). The incorporation of a conforming step between the impregnation with H_3PO_4 and the activation step allows the successful development of disc-shape monoliths without the use of a binder. Textural characterization results using N_2 adsorption at 77 K show that the effect of the activating agent highly depends on the nature of the carbon precursor used. While chemical activation with phosphoric acid has mainly no effect when using coconut shell, a large development of both micro- and mesoporosity is observed for African palm stones. Large concentrations of the activating agent produce the partial shrinkage of the narrow microporous structure independently of the precursor used. Concerning the adsorption of CO_2 at atmospheric pressure and 273 K, both series of activated carbon monoliths exhibit an improved adsorption behaviour with the activation degree up to an optimum value around ∼164 mg CO_2/g, for sample CACM-32, and ∼162 mg CO_2/g, for sample PACM-28, the amount adsorbed decreasing thereafter. Apparently, the total amount of CO_2 adsorbed under these experimental conditions is defined by the volume of narrow micropores (V_n).

Keywords Activated carbon monoliths · CO_2 adsorption · H_3PO_4 · Coconut shell · African palm stones

D.P. Vargas · L. Giraldo (✉)
Facultad de Ciencias, Departamento de Química,
Universidad Nacional de Colombia, Avenida Carrera 30
No. 45-03, Bogotá, Colombia
e-mail: lgiraldogu@bt.unal.edu.co

J. Silvestre-Albero
Departamento de Química Inorgánica, Universidad de Alicante,
Ap. 99, 03080 Alicante, Spain

J.C. Moreno-Piraján
Facultad de Ciencias, Departamento de Química,
Universidad de los Andes, Carrera 1 No. 18 A 10, Bogotá,
Colombia

1 Introduction

CO_2 capture using porous solids is becoming a challenging task owing to the increasing amount of CO_2 released to the atmosphere (mainly from power generation plants) and its impact in the global climate change (Karl and Trenberth 2003; Keeling et al. 1995; Steeneveldt et al. 2006). Zeolites, activated carbons, carbon molecular sieves (CMS), mesoporous silicas (e.g. MCM-41 and SBA-15) and, more recently, metal-organic framework materials (MOF) have shown promising results in terms of adsorption capacity and selectivity (Bae et al. 2008, 2009; Himeno et al. 2005; Inagaki 2009; Kapoor and Yang 1989; Wahby et al. 2010; Yazaydin et al. 2009). Furthermore, recent studies in this field have shown that the adsorption capacity of these porous solids for CO_2 can be improved by incorporation of nitrogen functional groups into their porous structure (Franchi et al. 2005; Huang et al. 2003; Pevida et al. 2008). Unfortunately, the incorporation of these functionalities has some disadvantages (e.g. cost, regeneration, slow CO_2 diffusion and so on); the development of new porous solids with improved properties in terms of adsorption capacity, selectivity and adsorption kinetics, avoiding post-synthesis modifications becomes a challenging task. Furthermore, besides achieving a large adsorption capacity and selectivity, an important aspect in the design of an adsorbent from an industrial point of view relates to the conforming step, i.e. pellets or monoliths are required instead of powders.

Among the different sorbents described before, carbon materials exhibit certain advantages such as low cost, high specific surface area and pore volume, high resistance to both acid and basic media and, more importantly, the possibility to tailor the textural properties and surface chemistry in order to improve the adsorption behaviour in a certain application (Marsh and Rodríguez-Reinoso 2006). Furthermore, carbon materials exhibit another advantage. They can be conformed either into pellets or monoliths without the use of a binder by appropriate selection of the carbon precursor (e.g. petroleum pitch) (Ramos-Fernández et al. 2008) or the activation treatment used during the synthesis (e.g. chemical activation with $ZnCl_2$ or H_3PO_4) (Nakagawa et al. 2007). In this sense, recent studies from Wahby et al. have shown that the appropriate selection of both the carbon precursor and the activation procedure used allows the development of carbon molecular sieves, either as a powder or as a monolith, with a large adsorption capacity for CO_2 (up to 383 mg CO_2/g sorbent) together with an optimum pore opening able to discriminate CO_2 from other side-products such as CH_4 and N_2 (Ramos-Fernández et al. 2008; Wahby et al. 2010).

With this in mind, the aim of this manuscript is the development of activated carbon monoliths from natural lignocellulosic precursors (coconut shell and African palm stones) using H_3PO_4 as activating agent. Interestingly, these monoliths will be synthesized without the use of a binder using the tars evolved during the impregnation step to consolidate the carbon grains (Nakagawa et al. 2007; Vargas-Delgadillo et al. 2010; Vargas et al. 2009). The performance of these activated carbon monoliths will be analyzed in the adsorption of CO_2 at 273 K and atmospheric pressure.

2 Experimental section

Two series of binderless activated carbon monoliths have been prepared from different lignocellulosic precursors (coconut shell and African palm stones) using H_3PO_4 as activating agent. Briefly, the precursors were crushed and sieved to a particle size of 0.038 mm and subsequently impregnated with a solution of H_3PO_4 for 2 h at 358 K. For both lignocellulosic precursors several concentrations of phosphoric acid (24 wt.%, 28 wt.%, 32 wt.%, 36 wt.% and 48 wt.%; 1 g of precursor for 2 ml of solution) were used in order to prepare series of monoliths denoted as CACM (coconut activated carbon monolith) and PACM (African palm activated carbon monolith) followed by the concentration used. After the impregnation step, samples were dried at 383 K for 2 h and subsequently conformed under pressure at 423 K and 45 MPa using a cylindrical mould with an internal diameter of 1.8 cm. The prepared monoliths were heat treated in a horizontal furnace up to 723 K for 2 h (heating rate 1 $K \cdot min^{-1}$) using a N_2 flow of 85 $ml \cdot min^{-1}$. Finally, the prepared monoliths were extensively washed with hot distilled water until neutral pH is achieved.

Textural properties of the synthesized monoliths were analyzed using N_2 adsorption measurements at 77 K in a volumetric system (Quantachrome, Autosorb 3-B). Before the adsorption experiments, samples were submitted to an outgassing treatment at 523 K for 4 h. The volume of micropores, $V_0(N_2)$, was obtained by application of the Dubinin-Radushkevich equation to the nitrogen adsorption data. The total pore volume, V_t, was obtained from the amount adsorbed at a relative pressure p/p_0 of 0.99 while the mesopore volume, V_{meso}, was obtained from the difference between the total pore volume and the micropore volume. Finally, the "apparent" surface area was obtained by application of the BET (Brunauer, Emmett and Teller) equation to the nitrogen adsorption data (Brunauer et al. 1938). Additionally, immersion calorimetry measurements into benzene (0.37 nm) were performed in a home-made calorimeter Calvet type (Giraldo et al. 2003; Moreno and Giraldo 2000).

The adsorption capacity for CO_2 in the different activated carbon monoliths at atmospheric pressure and 273 K was measured using a volumetric system (Quantachrome, Autosorb 3-B). Before the adsorption experiments, the different samples were outgassed at 523 K for 4 h. The volume of narrow micropores ($V_n(CO_2)$; pores <0.7 nm) was obtained by application of the Dubinin-Radushkevich equation to the CO_2 adsorption data.

3 Results and discussion

3.1 Sample characterization

Figure 1 shows schematic pictures of the different synthesized monoliths using either coconut shell or African palm stone as carbon precursor. As it can be observed, well-defined disc-shape carbon monoliths can be obtained without the use of a binder, independently of the carbon precursor used. The synthesized activated carbon monoliths have an external diameter of around 1.5 cm and a height of 8 mm.

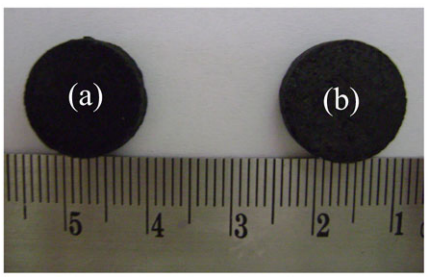

Fig. 1 Schematic picture of the different activated carbon monoliths, (**a**) CACM and (**b**) PACM

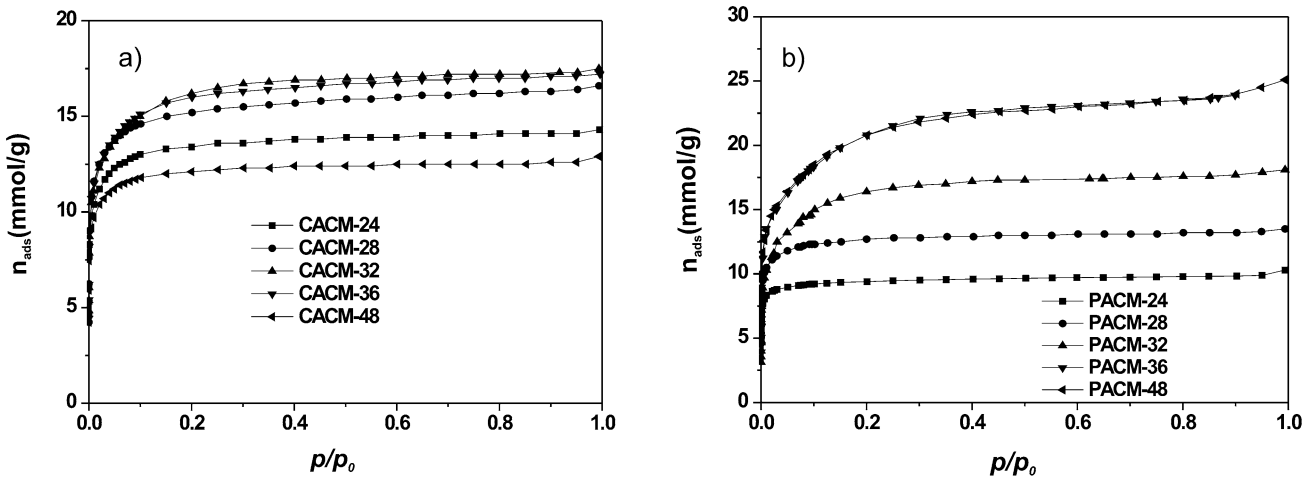

Fig. 2 Nitrogen adsorption isotherms for the two series of activated carbon monoliths, (**a**) CACM and (**b**) PACM, prepared using a different concentration of activating agent H_3PO_4 (24 wt.%, 28 wt.%, 32 wt.%, 36 wt.% and 48 wt.%)

Phosphoric acid (H_3PO_4) is a Brönsted acid and strong dehydrating agent which produces the evolution of tars during the impregnation step in such a way that these tars can be used to consolidate the carbon grains into monoliths by conforming under pressure, these monoliths having good mechanical rigidity. Furthermore, recent studies described in the literature have shown that the conforming step produces a narrowing of the existing micropores (compared to the powder counterpart) due to the plasticity of the precursor and, in addition, provides a lower interparticle space, which improves the adsorption capacity in a volumetric basis (Nakagawa et al. 2007; Vargas-Delgadillo et al. 2010).

The textural characteristics of the different activated carbon monoliths were measured using N_2 adsorption at 77 K. Figure 2 shows the nitrogen adsorption isotherms for the different series of samples, (a) CACM and (b) PACM. As it can be observed, the monoliths prepared using coconut shell as a carbon precursor are pure microporous materials with a narrow knee at low relative pressures ($p/p_0 < 0.1$) and a type I nitrogen isotherm, according to the IUPAC classification. For these samples, an increase in the concentration of activating agent (H_3PO_4) gives rise to an increase in the amount of nitrogen adsorbed together with a slight widening of the knee at low pressures. In any case, no mesoporosity is observed for these samples independently of the concentration of activating agent incorporated. A completely different behaviour is observed for the monoliths prepared using the same activation procedure but using African palm stones as a precursor. As it can be observed in Fig. 2b, while the sample prepared with 24 wt.% H_3PO_4 is a pure microporous sample, an increase in the proportion of activating agent gives rise to an important widening of the knee in the nitrogen adsorption isotherm, i.e. development of wide micropores together with the development of some mesopores for concentrations above 32 wt.%. This effect is confirmed by the presence of a significant slope in the nitrogen adsorption isotherm above $p/p_0 \sim 0.2$. These observations can be clearly observed in Table 1, where the different textural parameters have been summarized, and in Fig. 3 where the pore size distribution (PSD) for some representative samples is included. The pore size distribution has been obtained after application of the NLDFT model to the nitrogen adsorption data and assuming a slit-shape pore model.

As it can be observed in Table 1, the "apparent" surface area of the synthesized activated carbon monoliths ranges from 1150–1330 m^2/g, for samples prepared from coconut shell, and from 820–1640 m^2/g, for samples prepared from African palm stones. The larger differences in the BET surface area for samples PACM clearly shows that the activating agent exhibits a different effect depending on the characteristics of the original raw material. While coconut shell seems to be highly stable under these acidic conditions, i.e. depolymerisation of the constituents of the lignocellulosic precursor seems to be not highly effective; the same treatment gives rise to a high development of the porosity when African palm stones is used. Furthermore, the use of high concentrated H_3PO_4 has a detrimental effect on samples CACM (see for instance sample CACM-48) where a sudden shrinkage of the porosity is observed. A similar shrinkage of the narrow microporous structure has been described in the literature for activated carbon monoliths prepared from olive stones and using large concentrations of phosphoric acid as activating agent (Nakagawa et al. 2007).

As described before, the total micropore volume has been evaluated from the nitrogen adsorption data after application of the Dubinin-Radushkevich (DR) equation. At this point it must be highlighted that the application of the DR equation to the nitrogen adsorption data for both series of monoliths gives rise to two well-defined slopes, the first one between $\log^2(p_0/p) \sim 0.1$–2.0 and the second one between

Table 1 Textural parameters for the different activated carbon monoliths obtained from the N_2 and CO_2 adsorption data at 77 K and 273 K, respectively

N_2 adsorption data at 77 K					CO_2 adsorption data at 273 K
Sample	S_{BET} (m^2/g)	V_0 (cm^3/g)	V_{meso} (cm^3/g)	$V_{0.99}$ (cm^3/g)	V_n (cm^3/g)
CACM24	1150	0.44 (0.49)	0.05	0.49	0.39
CACM28	1295	0.50 (0.55)	0.08	0.58	0.44
CACM32	1322	0.49 (0.60)	0.11	0.61	0.42
CACM36	1331	0.50 (0.59)	0.10	0.60	0.41
CACM48	1045	0.40 (0.43)	0.04	0.45	0.32
PACM24	819	0.33	0.03	0.36	0.27
PACM28	1092	0.42 (0.45)	0.05	0.46	0.36
PACM32	1300	0.45 (0.57)	0.17	0.62	0.43
PACM36	1636	0.60 (0.75)	0.23	0.83	0.28
PACM48	1638	0.58 (0.74)	0.29	0.87	0.24

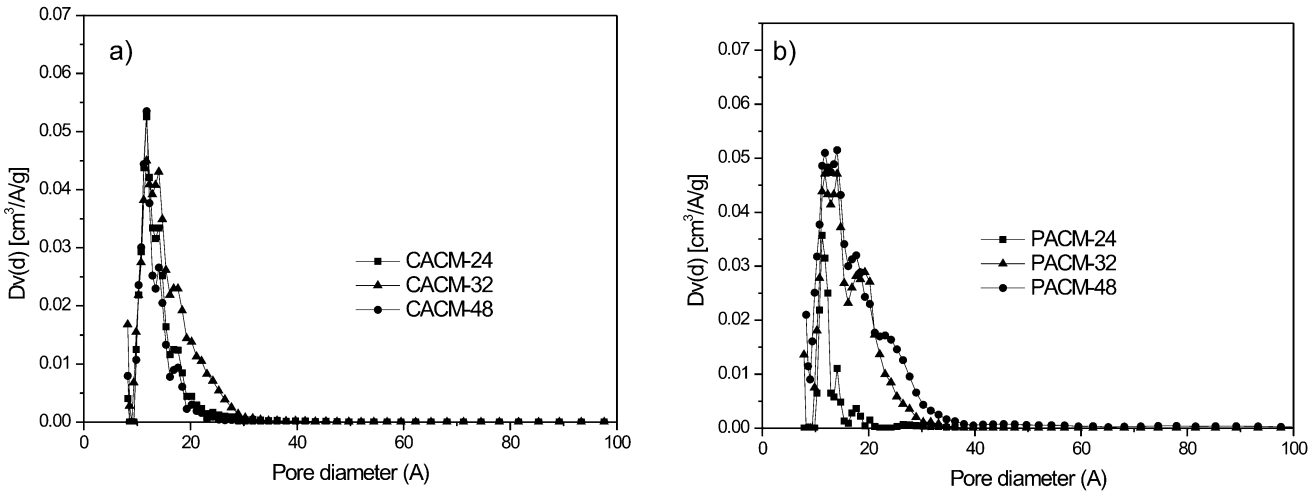

Fig. 3 Pore size distribution for (**a**) coconut shell and (**b**) African palm stones activated carbons after application of the NLDFT model to the N_2 adsorption data at 77 K (slit-shape pore model)

$\log^2(p_0/p) \sim 2.0$–10.0. These two values are included in Table 1, although only the second slope (between 2.0 and 10.0) has been used for the discussion in the subsequent sections (the first branch at low $\log^2(p_0/p)$ values has been included in brackets). A similar upward deviation at high relative pressures, i.e. low $\log^2(p_0/p)$ values, has been described in the literature for activated carbon prepared from olive stones and using physical activation with CO_2 (Garrido et al. 1987). The deviation observed for these samples above a certain burn-off, 52%, can be attributed to the presence of a bimodal pore size distribution. Additionally, Table 1 shows the volume of narrow micropores (V_n) obtained from the CO_2 adsorption data at 273 K after application of the Dubinin-Radushkevich equation. This value corresponds to the volume of pores below ~0.7 nm (Garrido et al. 1987). As it can be observed, for all samples the volume of narrow micropores (V_n) is always smaller than the total volume of micropores (V_0), i.e. while N_2 measures all micropores below 2 nm, CO_2 only measures the volume of pores below 0.7 nm. This behaviour reflects the absence of kinetic restrictions (narrow constrictions) for N_2 to access the narrow microporosity (Rios et al. 2007). However, the small differences between these two values for samples CACM clearly confirm the presence of a narrow micropores size distribution, in accordance with previous observations. A different situation occurs for samples PACM where the difference between V_n and V_0 is small for samples with a low activation degree while this difference increases with H_3PO_4 concentration, due to the development of larger micropores and mesopores.

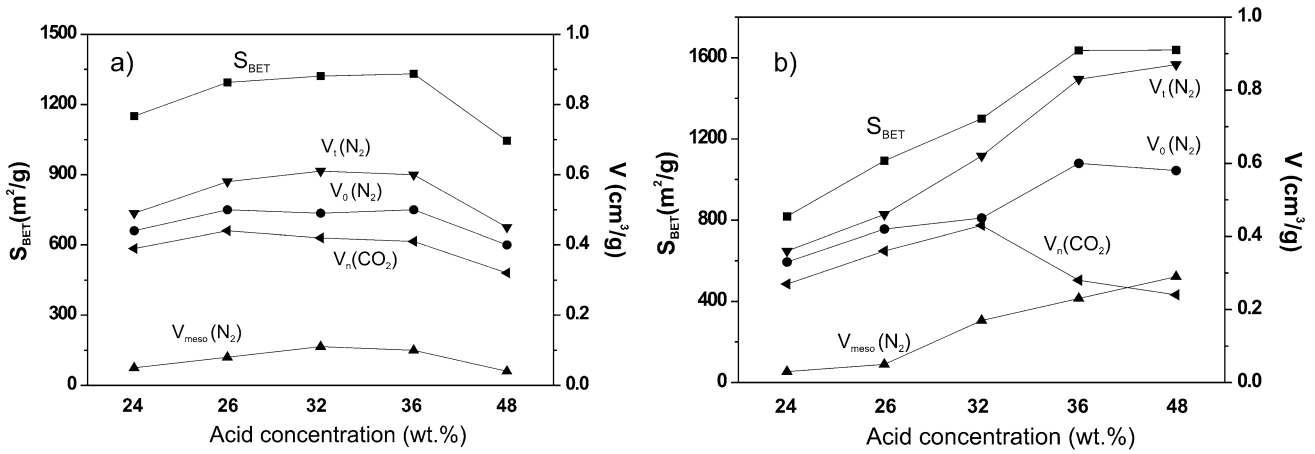

Fig. 4 Evolution of different sets of pore volume and BET surface area along activation with phosphoric acid for series (**a**) CACM and (**b**) PACM

The effect of the activating agent in the development of the porosity for each of the precursors used can be more clearly discerned by plotting the evolution of the different textural parameters as a function of the activation degree. In this sense, Fig. 4 shows the evolution of the S_{BET}, V_0, V_{meso}, $V_{0.99}$ and V_n as a function of the H_3PO_4 concentration used.

Figure 4 clearly shows that the effect of phosphoric acid as activating agent highly depends on the nature of the carbon precursor used. On samples prepared from coconut shell an increase in the concentration of phosphoric acid produce mainly no changes in the porous structure of the synthesized activated carbon probably due to the characteristics of the constituents of the lignocellulosic precursor, i.e. they are highly resistant to acidic media and depolymerization is not favoured. Only at high concentrations there is a sudden decrease both in surface area and pore volumes due to the partial shrinkage/destruction of the porous structure. Contrary to the behaviour with coconut shell, the effect of the activating agent is more effective when using African palm stones as carbon precursor. For a H_3PO_4 concentration below 26 wt.%, samples develop mainly narrow micropores as deduced by the constant difference between V_0 and V_n. Above 26 wt.%–32 wt.% there is a clear widening of the microporosity, i.e. total micropore volume (V_0) continues growing while narrow micropore volume (V_n) start to decline; mesopore volume (V_{meso}) also starts growing thereafter. Higher concentrations produce a further development of wide micropores and mesopores while narrow micropores drastically decrease probably due to the partial shrinkage/collapse of inner porous structure. Large concentrations of phosphoric acid promote the depolymerization of lignin, thus producing a decrease in the mechanical properties of the particles, and consequently, the swelling of the porous structure.

The textural characterization of the porous structure has been complemented by immersion calorimetry measurements into benzene, with a kinetic diameter of 0.37 nm. In the absence of specific interactions at the solid-liquid interface, the heat of immersion into a certain liquid can be used to evaluate the surface area available for this molecule, in such a way that using liquids with different molecular dimensions provides an estimation of the surface area available for each molecular size, i.e. the pore size distribution (Silvestre-Albero et al. 2001, 2009, 2010). In this sense, Table 2 shows the enthalpy of immersion ($-\Delta H_{imm}$) into benzene for the two series of activated carbon monoliths together with the accessible surface area obtained from the corresponding heat of immersion and using a non-porous graphitized carbon black (V3G; $S_{BET} = 62\ m^2/g$) as a reference sample.

Enthalpy of immersion into benzene is higher in samples prepared from coconut shell when compared to the same samples prepared from African palm stones in spite of the smaller BET surface area in the former samples. As it can be observed in Table 2, the total surface area accessible to benzene, estimated from the corresponding enthalpy values, are quite closed to the values obtained from N_2 adsorption at 77 K after application of the BET equation. This similarity confirms the high accuracy of the home-made immersion calorimetry equipment (Giraldo et al. 2003; Moreno and Giraldo 2000). When comparing the effect of the concentration of activating agent in both series there are important changes for samples with a high activation degree. In both cases, while the BET surface slightly decreases or even continuous increasing, the heat of immersion and the associated accessible surface area for benzene experiences a sudden decrease, this effect being more evident for highly activated samples prepared from African palm stones. This behaviour can be explained by the partial collapse/shrinkage of the porous structure for samples prepared using high concentrated H_3PO_4, as described before. Apparently, this effect is more sensible for a larger molecule such as benzene

Table 2 Enthalpy of immersion ($-\Delta H_{imm}$) into benzene for the different activated carbon monoliths together with the estimated total surface area accessible to benzene using a non-porous graphitized carbon black as a reference sample. "Apparent" surface area obtained after application of the BET equation is included for the sake of comparison

Sample	CACM24	CACM28	CACM32	CACM36	CACM48
$-\Delta H_{imm}$ (J/g)	120	130	132	145	113
S_{BZ} (m^2/g)	1054	1142	1300	1159	992
S_{BET} (m^2/g)	1150	1295	1322	1331	1045
Sample	PACM24	PACM28	PACM32	PACM36	PACM48
$-\Delta H_{imm}$ (J/g)	96	123	130	120	96
S_{BZ} (m^2/g)	843	1080	1142	1053	843
S_{BET} (m^2/g)	819	1092	1300	1636	1638

Table 3 Amount of CO_2 adsorbed (mg/g) at atmospheric pressure and 273 K for the different activated carbon monoliths prepared both from Coconut shell (CACM) and African palm stones (PACM) as a function of the activation degree

Sample	CACM24	CACM28	CACM32	CACM36	CACM48
mg CO_2/g	147	152	164	158	145
Sample	PACM24	PACM28	PACM32	PACM36	PACM48
mg CO_2/g	141	162	144	105	88

(0.37 nm for slit-shape pores and 0.56 nm for cylindrical pores) compared to nitrogen (0.36 nm). Most probably, in these samples the swelling of the porous structure is modifying the pore size and shape in such a way that the N_2 molecule is able to access the porosity while benzene experience kinetic restrictions.

3.2 Adsorption of CO_2 at 273 K

As described in the introduction, one of the main applications of activated carbons concerns gas adsorption/storage. CO_2 adsorption constitutes a challenging task due to environmental concerns, i.e. global climate change. In this sense, the ability of the synthesized activated carbon monoliths for CO_2 adsorption has been evaluated in a volumetric equipment at atmospheric pressure and 273 K (see Table 3).

As it can be observed, in both cases the amount of CO_2 adsorbed increases with the activation degree up to a maximum around 164 mg/g, in the case of the activated monoliths prepared from coconut shell, and 162 mg/g, in the case of the monoliths prepared from African palm stones. Independently of the carbon precursor used, the amount of CO_2 decreases thereafter for higher H_3PO_4 concentrations. Textural parameters described before showed that high concentrations of activating agent gave rise to several phenomena, i.e. the widening of the microporosity, development of mesoporosity and the partial destruction/shrinkage of the narrow microporous structure (breakdown of narrow micropores). From the results described in Table 3, it can be deduced that the partial shrinkage of the inner porous structure becomes detrimental for the CO_2 adsorption process. In order to clarify this hypothesis Fig. 5 correlates the amount of CO_2 adsorbed (mg/g) with the different textural parameters obtained using N_2 adsorption at 77 K and CO_2 adsorption at 273 K.

From Fig. 5 it is clear that the amount of CO_2 adsorbed in the two series of activated carbon monoliths can not be scaled with the "apparent" surface area or the total volume of micropores. In fact, samples PACM-36 and PACM-48 with an extremely large surface area (above 1600 m^2/g) and a large total micropore volume (V_0 above 0.58 cm^3/g) exhibit a poor adsorption behaviour for CO_2 at atmospheric pressure and 273 K. However, Fig. 5c shows that the total amount of CO_2 adsorbed exhibits a good correlation with the total volume of narrow micropores (V_n), deduced from the corresponding isotherms after application of the DR equation. Apparently, narrow micropores (pores below 0.7 nm) are responsible for the adsorption of a small molecule such as CO_2 (kinetic diameter 0.33 nm) under these experimental conditions. Similar correlations with the volume of narrow micropores has been described in the literature for the adsorption of a similar molecule (in a dimension basis) such as hydrogen (kinetic diameter 0.29 nm) into commercial carbon molecular sieves (Silvestre-Albero et al. 2009). The crucial role of the narrow microporosity in the adsorption of CO_2 at atmospheric pressure can explain the excel-

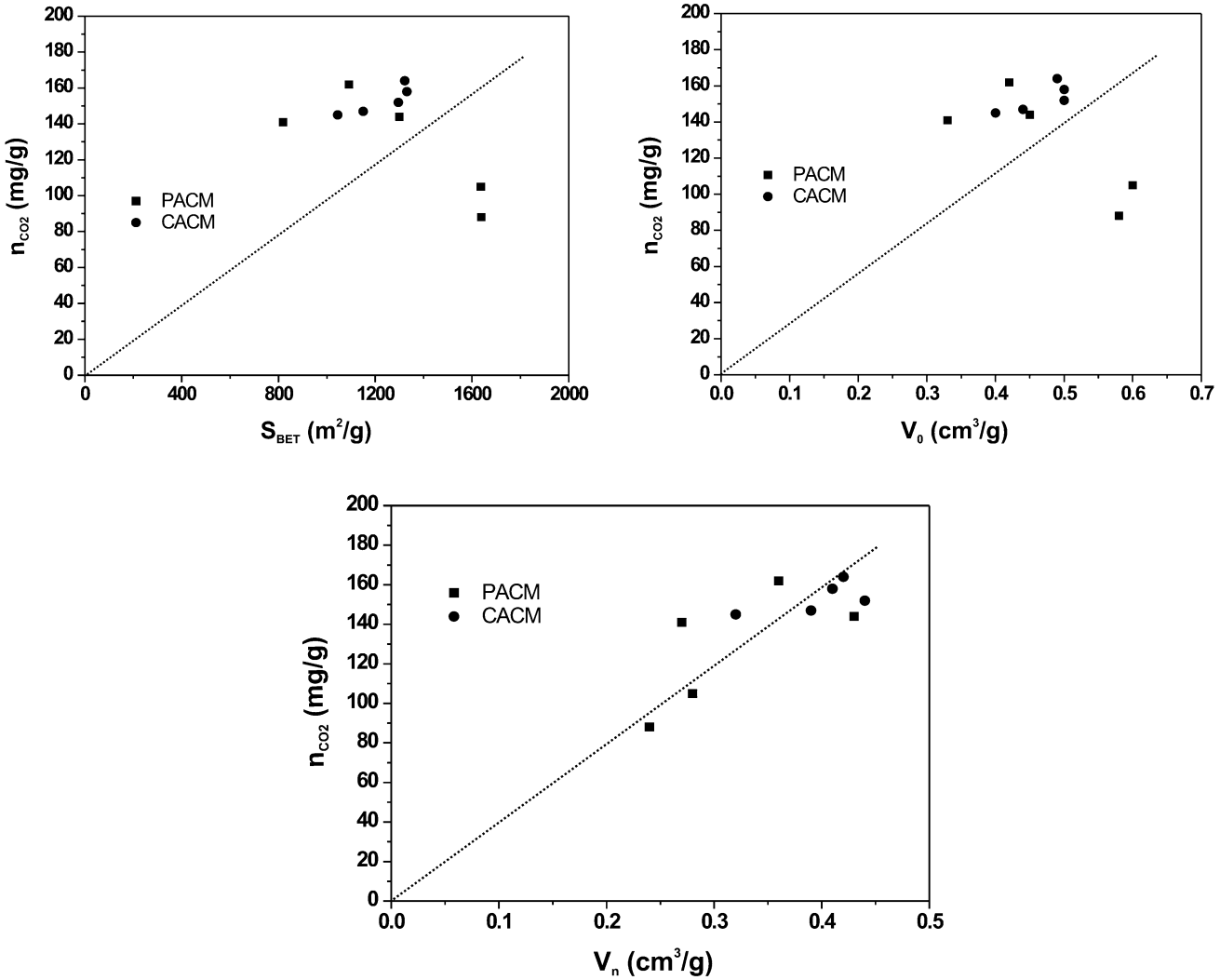

Fig. 5 Correlation between the amount of CO_2 adsorbed at atmospheric pressure and 273 K for the different activated carbon monoliths, and the different textural parameters (S_{BET}, $V_0(N_2)$ and $V_n(CO_2)$)

lent results recently described by Wahby and co-workers for CO_2 adsorption, with total amount adsorbed on high-surface area carbon molecular sieves (V_n above 1.40 cm^3/g) of ~380 mg CO_2/g, this value being even larger than those reported in the literature for traditional adsorbents such as zeolites and MOF materials (Bae et al. 2008, 2009; Himeno et al. 2005; Inagaki 2009, Kapoor and Yang 1989; Wahby et al. 2010; Yazaydin et al. 2009).

4 Conclusions

Two series of activated carbon monoliths have been prepared by impregnation of two lignocellulosic precursors, coconut shell and African palm stones, with phosphoric acid, followed by conforming under pressure and a thermal activation treatment at mild temperature. The confirming step before the thermal treatment allows the development of well-defined disc-shape monoliths due to the sintering ability of the tars evolved during the impregnation step with H_3PO_4. Experimental results show that the dehydrating effect of the chemical highly depends on the nature of the components of the lignocellulosic precursor. While phosphoric acid concentration has a small effect on the porous structure of the synthesized monoliths when using coconut shell as a precursor, a large development of wide micropores and mesopores is observed for African palm stones under similar experimental conditions. In both cases, large concentrations of the activating agent promote the swelling of the porous structure, thus producing the collapse/shrinkage of the narrow microporous network. Finally, adsorption experiments for CO_2 show that the amount adsorbed at atmospheric pressure and 273 K is mainly defined by the volume of narrow micropores (V_n). The total amount adsorbed achieves a maximum

of ∼164 mg/g, for sample CACM-32, and ∼162 mg/g, for sample PACM-28.

References

Bae, Y.-S., Farha, O.K., Spokoyny, A.M., Mirkin, C.A., Hupp, J.T., Snurr, R.Q.: Chem. Commun. 4135–4137 (2008)

Bae, Y.-S., Farha, O.K., Hupp, J.T., Snurr, R.Q.: J. Mater. Chem. **19**, 2131–2134 (2009)

Brunauer, S., Emmett, P.H., Teller, E.: J. Am. Chem. Soc. **60**, 309–319 (1938)

Franchi, R.S., Harlick, P.J.E., Sayari, A.: Ind. Eng. Chem. Res. **44**, 8007–8013 (2005)

Garrido, J., Linares-Solano, A., Martín-Martínez, J.M., Molina-Sabio, M., Rodríguez-Reinoso, F., Torregrosa, R.: Langmuir **3**, 76–81 (1987)

Giraldo, L., Huertas, J.I., Valencia, A., Moreno, J.C.: Instrum. Sci. Technol. **31**, 385–397 (2003)

Himeno, S., Komatsu, T., Fujita, S.: Adsorption **11**, 899–904 (2005)

Huang, H.Y., Yang, R.T., Chinn, D., Munson, C.L.: Ind. Eng. Chem. Res. **42**, 2427–2433 (2003)

Inagaki, M.: New Carbon Mater. **24**, 193–222 (2009)

Kapoor, A., Yang, R.T.: Chem. Eng. Sci. **44**, 1723–1733 (1989)

Karl, T.R., Trenberth, K.E.: Science **302**, 1719–1723 (2003)

Keeling, C.D., Whorf, T.P., Wahlen, M., Van der Plichtt, J.: Nature **375**, 666–670 (1995)

Marsh, H., Rodríguez-Reinoso, F.: Activated Carbon. Elsevier, London (2006)

Moreno, J.C., Giraldo, L.: Instrum. Sci. Technol. **28**, 171–178 (2000)

Nakagawa, Y., Molina-Sabio, M., Rodríguez-Reinoso, F.: Microporous Mesoporous Mater. **103**, 29–34 (2007)

Pevida, C., Plaza, M.G., Arias, B., Fermoso, J., Rubiera, F., Pis, J.J.: Appl. Surf. Sci. **254**, 7165–7172 (2008)

Ramos-Fernández, J.M., Martínez-Escandell, M., Rodríguez-Reinoso, F.: Carbon **46**, 384–386 (2008)

Rios, R.V.R.A., Silvestre-Albero, J., Sepúlveda-Escribano, A., Molina-Sabio, M., Rodríguez-Reinoso, F.: J. Phys. Chem. C **111**, 3803–3805 (2007)

Silvestre-Albero, J., Gómez-de-Salazar, C., Sepúlveda-Escribano, A., Rodríguez-Reinoso, F.: Colloids Surf., A, Physicochem. Eng. Asp. **187–188**, 151–165 (2001)

Silvestre-Albero, A., Wahby, A., Silvestre-Albero, J., Rodríguez-Reinoso, F., Betz, W.: Ind. Eng. Chem. Res. **48**, 7125–7131 (2009)

Silvestre-Albero, A., Ramos-Fernández, J.M., Martínez-Escandell, M., Sepúlveda-Escribano, A., Silvestre-Albero, J., Rodríguez-Reinoso, F.: Carbon **48**, 548–556 (2010)

Steeneveldt, R., Berger, B., Torp, T.A.: Chem. Eng. Res. Des. **84**, 739–763 (2006)

Vargas-Delgadillo, D.P., Giraldo, L., Moreno-Piraján, J.C.: E-J. Chem. **7**, 531–539 (2010)

Vargas, D.P., Giraldo, L., Moreno, J.C., Ladino, Y., Sapag, K.: In: Kaskel, S., Llewellyn, P., Rodríguez-Reinoso, F., Seaton, N.A. (eds.) Proceedings of the 8th International Symposium on the Characterization of Porous Solids, Cambridge, vol. 318, pp. 167–174 (2009)

Wahby, A., Ramos-Fernández, J.M., Martínez-Escandell, M., Sepúlveda-Escribano, A., Silvestre-Albero, J., Rodríguez-Reinoso, F.: ChemSusChem **3**, 974–981 (2010)

Yazaydin, A.O., Benin, A.I., Faheem, S.A., Jakubczak, P., Low, J.J., Willis, R.R., Snurr, R.Q.: Chem. Mater. **21**, 1425–1430 (2009)